The Astrophysical Journal, 788:99 (12pp), 2014 June 20 doi:10.1088/0004-637X/788/2/99

DISRUPTION OF A RED GIANT STAR BY A SUPERMASSIVE BLACK HOLE AND THE CASE OF PS1-10jh

Tamara Bogdanović[1,3,4], Roseanne M. Cheng[1,3], and Pau Amaro-Seoane[2,3]
[1] Center for Relativistic Astrophysics, School of Physics, Georgia Tech, Atlanta, GA 30332, USA; tamarab@gatech.edu, rcheng@gatech.edu
[2] Max Planck Institut für Gravitationsphysik (Albert-Einstein-Institut), D-14476 Potsdam, Germany; Pau.Amaro-Seoane@aei.mpg.de
Received 2013 July 22; accepted 2014 April 22; published 2014 May 28

ABSTRACT

The development of a new generation of theoretical models for tidal disruptions is timely, as increasingly diverse events are being captured in surveys of the transient sky. Recently, Gezari et al. reported a discovery of a new class of tidal disruption events: the disruption of a helium-rich stellar core, thought to be a remnant of a red giant (RG) star. Motivated by this discovery and in anticipation of others, we consider tidal interaction of an RG star with a supermassive black hole (SMBH) which leads to the stripping of the stellar envelope and subsequent inspiral of the compact core toward the black hole. Once the stellar envelope is removed the inspiral of the core is driven by tidal heating as well as the emission of gravitational radiation until the core either falls into the SMBH or is tidally disrupted. In the case of the tidal disruption candidate PS1-10jh, we find that there is a set of orbital solutions at high eccentricities in which the tidally stripped hydrogen envelope is accreted by the SMBH before the helium core is disrupted. This places the RG core in a portion of parameter space where strong tidal heating can lift the degeneracy of the compact remnant and disrupt it before it reaches the tidal radius. We consider how this sequence of events explains the puzzling absence of the hydrogen emission lines from the spectrum of PS1-10jh and gives rise to its other observational features.

Key words: accretion, accretion disks – black hole physics – galaxies: nuclei

Online-only material: color figures

1. INTRODUCTION

A star whose orbit takes it on a close approach to a supermassive black hole (SMBH) will be torn apart when the SMBH's tidal force is comparable to the self-gravity of the star (Rees 1988). The subsequent accretion of stellar debris by the SMBH generates a characteristic flare of UV and soft X-ray radiation, a signature which for nearly two decades has been used as a strong diagnostic for the presence of an SMBH in a previously inactive galaxy (Grupe et al. 1995a, 1995b, 1999; Renzini et al. 1995; Bade et al. 1996; Komossa & Greiner 1999; Greiner et al. 2000; Donley et al. 2002; Li et al. 2002; Komossa et al. 2004; Gezari et al. 2006, 2008, 2009; van Velzen et al. 2011, etc.). For many of the observed candidates, the appearance of the flare and its properties can be explained by an encounter of a main sequence star with the SMBH, which is expected to be the most common disruption scenario because of the relative abundance of this population of stars. More recently, however, the improved observational coverage of the transient sky led to discoveries of new classes of tidal disruption events.

One such event (PS1-10jh) was reported by Gezari et al. (2012) as a disruption of a helium-rich stellar core, thought to be a remnant of a red giant (RG) star. PS1-10jh shares some common properties with previously detected candidates which supports its identification as a tidal disruption, but also exhibits differences which may be a key to understanding the physical processes at play. For example, a well-sampled UV light curve of PS1-10jh is in agreement with the canonical theoretical expectation that the luminosity of a tidal disruption event should decay as $\propto t^{-5/3}$ (Rees 1988; Evans & Kochanek 1989).[5] The optical spectrum of the event is characterized by the presence of relatively broad He II emission lines, a property which is unusual given the absence of broad hydrogen emission lines. Both sets of emission lines are commonly found in the spectra of active galactic nuclei (AGNs), where hydrogen Balmer lines typically dominate in strength because of the higher abundance of hydrogen relative to helium in the interstellar medium. In light of this, Gezari et al. (2012) interpreted the optical spectrum of PS1-10jh as the emission from the disrupted He core of an RG star which lost its hydrogen envelope at some earlier point in time. Similar interpretation was provided by Wang et al. (2011, 2012), who discovered another tidal disruption candidate with strongly blueshifted He II emission line and weak hydrogen lines in their sample of extreme coronal line emitters.

Indeed, a tenuous outer envelope can be tidally stripped from the progenitor RG star at relatively large distances from the SMBH and before its compact core is disrupted or swallowed. This implies that the hydrogen envelope debris in the aftermath of disruption can be distributed over a wide range of spatial scales (in some cases comparable to the size of the broad line region (BLR)). Consequently, like the BLR, it is expected to be characterized by a range of ionization parameters—a state which in general does not preclude emission of hydrogen lines. Hence, one of the intriguing questions about PS1-10jh is what happened to its hydrogen envelope?

In this paper we adopt a premise that tidally disrupted star was an RG and investigate how this assumption constrains the orbital parameters and structure of the star that fell toward the black hole. Specifically, we consider scenarios that can result in early

[3] Visitor at the Kavli Institute for Theoretical Physics, University of California, Santa Barbara, CA.
[4] Alfred P. Sloan Research Fellow.

[5] The power-law behavior of tidal disruption light curves has however been predicted to vary as a function of time and emission wavelength (Lodato et al. 2009; Lodato & Rossi 2011).

separation and subsequent accretion of the hydrogen envelope of the star, so that at a later point in time when its helium core is disrupted, helium dominates the emission line spectrum. It is worth noting that this is not the only theoretical scenario put forward to explain the nature of PS1-10jh. Guillochon et al. (2014) propose that the emission-line spectrum of PS1-10jh may be produced in the disruption of a low-mass main sequence star. In this case, the debris from the disrupted star forms a compact BLR that consists of hydrogen-rich gas, but is highly ionized and effectively behaves as an H II region. Consequently, in this scenario it emits weak hydrogen emission lines below the current detection threshold.

An interesting property of RG encounters with SMBHs is that they can lead to partial disruptions with a surviving compact core. In scenarios where the stellar core is deposited deep in the potential well of the SMBH its dynamics will be affected by the relativistic precession of the pericenter, precession of the orbital plane due to the spin of the SMBH, and emission of gravitational waves (GWs). A stellar compact object that gradually spirals into an SMBH is commonly referred to as the extreme mass-ratio inspiral (EMRI). GW emission from EMRIs will only be detected by a future space-based grantational wave interferometer (e.g., Amaro-Seoane et al. 2013a). Nevertheless, if relativistic effects leave a visible imprint in the EM signatures of the disruption event, they can in principle be used to place independent constraints on the structure of the star and mass and spin of the SMBH (Gomboc & Čadež 2005; Kesden 2012a, 2012b) many years in advance of such GW observatory.

More generally, RG tidal disruptions are unique among stellar disruption scenarios because they can in principle serve as a tracer of a wide range of SMBHs. This is because the low density RG envelope can be tidally stripped even by the most massive of black holes which swallow, rather than disrupt main sequence and compact stars. Indeed, RGs are expected to make up a dominant fraction of the stellar diet for SMBHs with mass $\gtrsim 10^8\,M_\odot$ and about 10% of it for black holes below this threshold (MacLeod et al. 2012). They are also expected to contribute significantly to the duty cycle of low-level activity of SMBHs with mass $>10^7\,M_\odot$ (MacLeod et al. 2013). While disruptions of main sequence stars by $\sim 10^6\,M_\odot$ SMBHs will continue to dominate the detection rates, a growing observational sample of tidal disruption events indicates that more RG disruptions are likely to be observed in the future.

In this work we consider a partial disruption scenario where the stripping of the hydrogen envelope is followed by the subsequent inspiral and possible disruption of the compact remnant. In the case of PS1-10jh we find a set of orbital solutions where tidal interaction with an SMBH leads to the inspiral and disruption of the helium core after the accretion of the hydrogen envelope has been completed. Such configuration can provide an explanation for the lack of hydrogen emission signatures in the spectrum of PS1-10jh and places strong constraints on the dynamical evolution and structure of the core.

The remainder of this paper is organized as follows. In Section 2, we describe the stripping of the RG envelope and give the physical properties of the debris in Section 3. We consider the inspiral of the remnant core into the SMBH in Section 4, discuss implications for the disruption candidate PS1-10jh in Section 5, and conclude in Section 6.

2. TIDAL STRIPPING OF THE RED GIANT ENVELOPE

Consider a relatively common, low-mass RG star with a zero-age main sequence mass of $M_* = 1.4\,M_\odot$ and radius $R_* \approx 10^{12}$ cm.[6] This class of RG stars consists of a degenerate helium core, $M_{\rm core} \approx 0.3\,M_\odot$ and $R_{\rm core} \approx 10^9$ cm, and a hydrogen-rich envelope with mass $M_{\rm env} \approx 1.1\,M_\odot$, where the mass and size of the RG core are consistent with the structure of low-mass helium white dwarfs (Hamada & Salpeter 1961; Althaus & Benvenuto 1997). An RG star of this mass spends few $\times\ 10^8$ yr on the RG branch of the Hertzsprung–Russell diagram and transitions onto the horizontal branch after the ignition of the helium core in the event known as the helium flash.

The conditions for the tidal disruption of a star are fulfilled at the tidal radius, $R_T \approx R_*(M/M_*)^{1/3}$, where M is the mass of the black hole (Rees 1988). The tenuous and spatially extended stellar envelope renders RG stars particularly vulnerable to tidal forces, resulting in tidal radii $\sim$100 times larger than for main sequence stars,

$$R_T \approx 10^{14}\,{\rm cm}\left(\frac{R_*}{10^{12}\,{\rm cm}}\right)\left(\frac{M_*}{1\ M_\odot}\right)^{-1/3} M_6^{1/3}. \quad (1)$$

In terms of gravitational radii,

$$R_T \approx 680\,r_g\left(\frac{R_*}{10^{12}\,{\rm cm}}\right)\left(\frac{M_*}{1\ M_\odot}\right)^{-1/3} M_6^{-2/3}, \quad (2)$$

where $M_6 = M/10^6\,M_\odot$ and $r_g = GM/c^2 = 1.48 \times 10^{11}\,{\rm cm}\,M_6$. More specifically, this disruption radius is defined for a gas cloud whose density is equal to the mean density of an RG star. Since the mean density of the RG star is comparable to that of its hydrogen envelope, Equations (1) and (2) provide a good estimate for the distance from the SMBH where the stellar envelope will be stripped by the tides. On the other hand, a white dwarf-like core can survive the tidal forces of a million solar mass black hole even at separations comparable to the radius of its event horizon (equal to $2r_g$ for non-rotating black holes).

For a star on an orbit with pericentric distance R_p, the strength of the tidal encounter is characterized by the penetration factor $\beta = R_T/R_p$, where $\beta = 1$ marks the threshold for tidal disruption and $\beta \gg 1$ characterizes deep encounters (Carter & Luminet 1982). Similarly, the penetration factor for the RG core is defined as

$$\beta_{\rm core} = \beta\left(\frac{R_{\rm core}}{R_*}\right)\left(\frac{M_*}{M_{\rm core}}\right)^{1/3}. \quad (3)$$

For the core under consideration, $\beta_{\rm core} \approx \beta/600$. The core of finite extent experiences the gradient of the SMBH gravitational potential which at pericenter leads to a spread in the specific gravitational potential energy across the core's radius of $\Delta\epsilon_{\rm core} \approx GMR_{\rm core}/R_p^2$ (Lacy et al. 1982; Evans & Kochanek 1989, etc.). Recent calculations however show that for disruptive, $\beta > 1$ events the energy spread of the debris remains frozen at the point of disruption and is a very weak function of β (Stone et al. 2013; Guillochon & Ramirez-Ruiz 2013). This implies that the envelope which disrupts at $\sim R_T$ has energy spread $\Delta\epsilon_{\rm env} \approx GMR_*/R_T^2$. For nearly parabolic orbits the most bound portion of the envelope debris is characterized by $\epsilon = -\Delta\epsilon_{\rm env}$ and shortest Keplerian orbital period

$$P_{\rm m} \approx 2 \times 10^8\,{\rm s}\left(\frac{R_*}{10^{12}\,{\rm cm}}\right)^{3/2}\left(\frac{M_*}{1\,M_\odot}\right)^{-1} M_6^{1/2}. \quad (4)$$

[6] MacLeod et al. (2012) have recently modeled the dynamics of a red giant of this structure during one partially disruptive encounter with a supermassive black hole.

Assuming the distribution of debris mass over energy is approximately symmetric, $M_*/d\epsilon \approx f M_*/(2\Delta\epsilon)$ (Evans & Kochanek 1989), it is possible to derive the accretion rate of the debris bound to the SMBH

$$\dot{M} = \frac{dM_*}{d\epsilon}\frac{d\epsilon}{dt} = \frac{f\,M_*}{3P_{\rm m}}\left(\frac{t}{P_{\rm m}}\right)^{-5/3} \approx 0.054\,M_\odot\,{\rm yr}^{-1} \times f\left(\frac{R_*}{10^{12}\,{\rm cm}}\right)^{-3/2}\left(\frac{M_*}{1\,M_\odot}\right)^{2} M_6^{-1/2}\left(\frac{t}{P_{\rm m}}\right)^{-5/3}, \quad (5)$$

where f is the fraction of the RG stellar envelope that is accreted relative to the mass of the star.

MacLeod et al. (2012) used three-dimensional hydrodynamic simulations to model the fraction of the RG stellar envelope lost to tidal stripping as a function of the penetration factor of the encounter. They find that for $\beta = 1$ encounters the mass loss for a $1.4\,M_\odot$ RG star amounts to about $0.4\,M_\odot$, while for moderately deep $\beta \geqslant 2$ encounters it asymptotes to $0.7\,M_\odot$. The rest of the stellar envelope remains gravitationally bound to the core. For nearly parabolic orbits approximately half of the stripped envelope is launched toward the black hole while a comparable fraction is unbound and ejected from the system. It follows that after the most tightly bound debris completes its first orbit, the half that is bound to the SMBH will begin forming an accretion disk of mass ~0.2–0.35 $M_\odot$.

In this work we focus on RG stars on nearly radial initial orbits with eccentricities close to unity. This choice is motivated by the prediction of the loss cone theory that most of the stars on disruptive orbits originate from the sphere of gravitational influence of the SMBH or beyond (Magorrian & Tremaine 1999; Wang & Merritt 2004),

$$r_h = \frac{GM}{\sigma^2} = 1.3\times10^{18}\,{\rm cm}\left(\frac{\sigma}{100\,{\rm km\,s^{-1}}}\right)^{-2} M_6, \quad (6)$$

where σ is the stellar velocity dispersion. In the absence of any other effects which could modify stellar orbits, this implies that tidal stripping of the RG envelopes is important for stars with orbital eccentricities $1-e \lesssim R_T/r_h \sim 10^{-4}$ (see, however, Section 4.1 for discussion of dynamical processes that are expected to affect RG orbits).

Note that if the RG star is initially placed on a less eccentric orbit around the black hole, more than ~50% of its debris ends up bound to the SMBH, placing an upper limit on the mass of the accretion disk as $0.7\,M_\odot$. The disruption of stars on lower eccentricity orbits will also result in the return of debris to pericenter on timescales shorter than given by Equation (4) and consequently peak accretion rates larger than shown in Equation (5) (Hayasaki et al. 2013; Dai et al. 2013).

3. EMISSION PROPERTIES OF THE DEBRIS

It is worth noting that the envelope loss described above takes place at the point where the orbital radius of the star is comparable to R_T, which, for $\beta > 1$ encounters, occurs before the pericentric passage. As the RG remnant (i.e., stellar core plus the portion of the envelope bound to it) continues to approach pericenter, its self gravity continues to diminish relative to the tidal force of the black hole until the point of pericentric passage after which the trend reverses (Carter & Luminet 1982; Stone et al. 2013). The consequence of this reversal, combined with the rotation of the spun up core, is that the lobes which are nearly unbound from the remnant fold around and crash down on the core (R. M. Cheng et al. 2014, in preparation). This drives strong shocks in the outer layers of the remnant. In order to estimate an upper limit on the thermal energy produced by shocks and deposited onto the star during its pericentric passage, we assume that it is comparable to the binding energy of the envelope that crashes back onto the RG remnant. From results of MacLeod et al. (2012), the fraction of the total envelope mass $\eta M_{\rm env}$ that contracts back to the star is about $\eta = 0.1$ and at most 0.2 for deeper encounters.

If all of this material is shock-heated, the maximum amount of thermal energy produced can be estimated as $E_{\rm th} \approx \eta G M_* M_{\rm env}/R_*$. Since the envelope has a large optical depth due to Thomson scattering, $\tau_T \approx 3\eta\, M_{\rm env}\,\sigma_T/(4\pi m_p R_*^2) \approx 2\times10^7$, in this scenario the thermal energy is radiated gradually over the diffusion timescale $t_{\rm diff} \sim \tau_T R_*/c \approx 7\times10^8$ s. The resulting luminosity of the flare is then

$$L_{\rm th} \sim \frac{E_{\rm th}}{t_{\rm diff}} \approx 4\times10^{37}\,{\rm erg\,s^{-1}}\left(\frac{M_*}{1\,M_\odot}\right). \quad (7)$$

A characteristic blackbody temperature of the shocked star and emitted radiation can be estimated from $\sigma T^4 = L_{\rm th}/4\pi R_*^2$ and is about $kT \sim 1$ eV for the RG properties considered here. Therefore, in the case of the RG tidal disruption, the shock from the fallback of nearly unbound material from the tidal tails leads to an initial optical flare, softer than ~1 keV flare expected from a completely disrupted main sequence star and considerably less energetic than expected from the full disruption of a white dwarf by an intermediate-mass black hole (Kobayashi et al. 2004). This emission arises in advance of the flare powered by the accretion of the debris onto the SMBH. In the case of the RG star considered here, it lasts for about 20 yr and thus cannot really be considered a "flare" as long as the slow diffusion processes determine the timescale for emission of the thermal energy. In reality, not all of the thermal energy produced in the fallback would be radiated and some of it would be deposited into the remnant, so the estimated luminosity in Equation (7) should be considered as an upper limit.

Additional emission arises from the envelope debris which falls back toward the SMBH and starts forming an accretion disk. The debris bound to the hole, initially distributed over a range of highly eccentric orbits, will circularize once the orbits are closed. The conservation of angular momentum implies that the debris circularizes at a radius equal to twice its initial disruption radius, which in the case of the RG envelope is $a \approx 2R_T$. This simple estimate is supported by hydrodynamic simulations that follow the early evolution of the debris disk (Hayasaki et al. 2013). Because shocks are localized to "intersection points" of the debris streams, the radiation emitted in this process encounters a relatively small column of matter and should escape to infinity without significant reprocessing by the intervening debris. We thus assume that the energy released during the circularization will be promptly emitted as radiation. From conservation of angular momentum, it is possible to show that the amount of orbital energy released during circularization is $\Delta E_{\rm circ} \approx GMM_{\rm disk}(2e-1)/(4R_T) \approx GMM_{\rm disk}/(4R_T)$, where $e \to 1$ is the initial orbital eccentricity of the debris. The luminosity produced during circularization is then

$$L_{\rm circ} \sim \frac{\Delta E_{\rm circ}}{P_{\rm m}} = 7\times10^{41}\,{\rm erg\,s^{-1}} \times\left(\frac{R_*}{10^{12}\,{\rm cm}}\right)^{-5/2}\left(\frac{M_*}{1\,M_\odot}\right)^{4/3}\left(\frac{M_{\rm disk}}{0.2\,M_\odot}\right) M_6^{1/6}, \quad (8)$$

where $M_{\rm disk}$ is the mass of the debris disk, corresponding to the amount of the stellar envelope that remains bound to SMBH (see discussion at the end of Section 2).

We next consider the fraction of luminosity contributed by the fall-back of debris from the circular orbit with the average radius of $\sim 2R_T$, all the way to the innermost stable circular orbit (ISCO) of the SMBH. Note that in reality circularization and inspiral of the debris play out concurrently rather than in sequence but we consider the two processes separately in order to estimate their individual luminosity budgets. Initially, the luminosity of the accretion flow increases with time as the radiative efficiency of the debris that inspirals toward ISCO increases,

$$L_{\rm fb} = \epsilon(r)\,\dot{M}c^2 \approx 2\times 10^{44}\,{\rm erg\,s^{-1}}\,f\,\left(\frac{\epsilon}{0.057}\right) \times \left(\frac{R_*}{10^{12}\,{\rm cm}}\right)^{-3/2}\left(\frac{M_*}{1\,M_\odot}\right)^{2} M_6^{-1/2}\left(\frac{t}{P_{\rm m}}\right)^{-5/3}, \quad (9)$$

where $\epsilon = 1-(r-2)/(r(r-3))^{1/2}$ is the radiative efficiency for a Schwarzschild black hole and r is the orbital radius of the debris in units of r_g (for, e.g., Frank et al. 2002). For $r = 2R_T$ and R_T given by Equation (2), radiative efficiency is only $\epsilon \approx 4\times 10^{-4}$ and it gradually increases to 0.057 as material reaches ISCO, which is located at $6r_g$ for a non-rotating black hole. Therefore, with the exception of the early stages of circularization when the low radiative efficiency results in a lower fall-back luminosity, at most times $L_{\rm fb} \gg L_{\rm circ} \gg L_b$. According to Equation (9), at ISCO the debris reaches its peak luminosity which for low-mass SMBHs is comparable to their Eddington luminosity.[7] This implies that radiative pressure can play an important role in limiting the luminosity of such systems.

The temperature of the debris radiating at the Eddington limit from the radius $\sim 2R_T$ is (Ulmer 1999)

$$T_{\rm eff} \approx \left(\frac{L_{\rm Edd}}{16\pi R_T^2\sigma}\right)^{1/4} = 4.6\times 10^4\,{\rm K}\left(\frac{R_*}{10^{12}\,{\rm cm}}\right)^{-1/2}\left(\frac{M_*}{1\,M_\odot}\right)^{-1/6} M_6^{1/12}, \quad (10)$$

where σ is the Stefan–Boltzmann constant. As material finds itself deeper in the potential well of the black hole, the temperature of the emitted multi-temperature blackbody radiation increases by a factor of $(2R_T/6r_g)^{1/2}$, or about 15 times for the scenario considered here. Therefore, the temperature evolution of the radiation emitted during the fall-back phase can in principle be used to infer the radiative efficiency of the debris disk at different radii from the SMBH. In practice, however, the emitted radiation is likely to be reprocessed by the debris material and emerge as radiation of lower temperature. This occurs because the debris disk with radius $\sim 2R_T$ has a significant optical depth, $\tau_T \approx M_{\rm disk}\,\sigma_T/2\pi(2R_T)^2 m_p \approx 730$. Nevertheless, if the broad emission line profiles (such as FeKα or hydrogen Balmer lines) are available from spectroscopic observations for this early phase of disruption before the luminosity peak, their width and shape can be used to constrain the radius of the inspiralling debris independently from its temperature.

The evolution of optical depth of the debris in the scenario considered here implies that the debris disk will become transparent to radiation once it expands by a factor of ~ 27 due to the transport of angular momentum. The conservation of angular momentum implies that at this point in time the mass of the disk will be $\sim M_{\rm disk}/\sqrt{27}$, after about 80% of its mass has been accreted onto the black hole. Assuming the accretion rate given by Equation (5), for a $\beta = 1$ encounter of a $1.4\,M_\odot$ RG with a $10^6\,M_\odot$ SMBH and $M_{\rm disk} = 0.2\,M_\odot$ this amount of debris is accreted only $t_{\rm acc} \sim$ few $\times\ P_{\rm m}$ after the luminosity peak, at which point the character of the debris disk emission changes to optically thin. In this simple estimate we only consider the fall-back accretion rate and direct the reader to a recent work by Shen & Matzner (2014) for a careful treatment of evolution of transient disks that form in tidal disruptions.

[7] Eddington luminosity is defined as $L_{\rm Edd} \approx 1.3\times 10^{44}\,{\rm erg\,s^{-1}}\,M_6$.

4. INSPIRAL OF THE COMPACT CORE INTO A SUPERMASSIVE BLACK HOLE

We now estimate the orbital properties of the surviving stellar remnant given a range of initial orbits as a function of the penetration factor and orbital eccentricity. The range of penetration factors considered here corresponds to the orbital pericenters between the ISCO (where the core plunges into the SMBH) and R_T (where the RG star loses its envelope). For Schwarzschild black holes of different masses this range corresponds to

$$\begin{aligned} 10^6\,M_\odot &: R_p \approx 9\times 10^{11} - 10^{14}\,{\rm cm} \\ 10^7\,M_\odot &: R_p \approx 9\times 10^{12} - 2\times 10^{14}\,{\rm cm} \\ 10^8\,M_\odot &: R_p \approx 9\times 10^{13} - 5\times 10^{14}\,{\rm cm}. \end{aligned} \quad (11)$$

The mechanisms that potentially determine the orbital evolution of the RG remnant in this phase are: (1) the interactions with the stars in the nuclear star cluster, (2) tidal interaction with the SMBH, (3) emission of GWs, and (4) gravitational and hydrodynamical interaction with the disk formed from the envelope debris.

4.1. Orbital Dynamics of the Core in the Galactic Nucleus

Stars on highly eccentric orbits can venture far from the central SMBH and experience a gravitational influence of other stars in the nuclear cluster at apocenter, where gravitational influence of the SMBH is at the minimum. Their orbital energy and angular momentum changes as a consequence of these interactions and therefore it is necessary for such spatially extended orbits to consider the contribution of the cluster stars to the gravitational potential of the central SMBHs.

In crowded stellar environments, in the centers of nuclear star clusters, the initial energy and angular momentum of an RG star can also be altered by physical collisions with other stars (Frank & Rees 1976). Collisions between RGs and stellar mass black holes have indeed been suggested as a plausible mechanism that can deplete the low-mass giants and asymptotic giant branch stars in the mass range 1–3 $M_\odot$ within the 0.4 pc radius in the Galactic Center (Dale et al. 2009; Davies et al. 2011). These studies indicate that the probability that an RG star will encounter a stellar mass black hole (or with a lesser probability a main sequence star) at least once during its lifetime is substantial. Specifically, as the stellar black hole passes close to the RG, the core is deflected from its original orbit retaining some fraction of the envelope. A scattering (and even more so a physical collision) with a massive perturber can, however, lower the initial eccentricity of the RG orbit and place it on a bound orbit around the SMBH, even if it initially originated beyond the sphere of gravitational influence of the SMBH (Perets et al.

2009). We thus conjecture that the RG remnant underwent such an interaction and consider its end as a starting point of our investigation, given that the RG remnant has been deflected onto a new orbit with the pericenter in the range given by Equation (11) and an arbitrary apocenter somewhere within r_h (Equation (6)).

We borrow from the investigations of EMRIs to elucidate the necessary conditions for an RG remnant to spiral in close to the SMBH where it can be disrupted or become a source of GWs. EMRI studies indicate that the evolution of compact objects with the range of pericenters shown in Equation (11) is dominated by a combination of relativistic precession effects, GW energy loss, but also vectorial resonant relaxation and two-body relaxation (Amaro-Seoane et al. 2013b). Recent work on stellar dynamics has shown that the formation rate of EMRIs sensitively depends on their eccentricity. For example, the rates of the EMRIs with semi-major axes $a_{\rm sb} \sim 10^{15}\,{\rm cm}\,(1-e^2)^{-1/3}$ can be strongly suppressed by the presence of what is usually referred to as the Schwarzschild barrier (Merritt et al. 2011; Brem et al. 2014). This barrier is a consequence of relativistic precession, which becomes pronounced as the compact object finds itself sufficiently deep in the potential well of the SMBH. The precession effectively blocks the gravitational influence of cluster stars that would otherwise build up over many approximately coherent orbits (Rauch & Tremaine 1996) and drive compact objects into the GW dominated regime. In the context of the RG remnant the relevant question is: can the core continue to spiral in toward the SMBH given the presence of the Schwarzschild barrier? Along similar lines, vectorial resonant relaxation has been found to change the orientation of the stellar orbit relative to the SMBH spin, causing the compact object that was initially outside of the ISCO at one instance of time to plunge into the black hole in the next, thus limiting any tidal disruption or GW signal.

It has been shown that stellar objects with $a > a_{\rm sb}$, on highly eccentric orbits can evolve into EMRIs or tidal disruptions without danger of premature plunge into the SMBH or blockage by the Schwarzschild barrier (Merritt et al. 2011; Brem et al. 2014; Amaro-Seoane et al. 2013b). We use this criterion to further constrain the orbit of the RG remnant. For these objects, the two-body relaxation and emission of gravitational radiation remain the main drivers of orbital evolution. Which mechanism dominates is determined by the density and distribution of stars in the nuclear star cluster, the mass of the SMBH, and the initial orbit of the RG core.

The two-body relaxation is a diffusive (random walk) process resulting from small-angle gravitational scattering following the encounter of two stars (Chandrasekhar & Bok 1942), which can change both the orbital energy and angular momentum of the scattered star. The relaxation in angular momentum occurs on a timescale that is $(1-e^2)$ times shorter than that for the energy, implying that stars on very eccentric orbits can significantly change their eccentricity while maintaining approximately the same semi-major axis (Amaro-Seoane et al. 2012). In the case of an RG remnant which is undergoing two-body scattering close to the apocenter of its orbit, this would cause the pericentric distance to change. Since we are interested in following the cores that approximately maintain their pericentric radius over multiple passages by the SMBH, we need to determine which orbits are likely to be affected by two body relaxation as opposed to the emission of GWs.

We use Equation (6) from Amaro-Seoane et al. (2012) and estimate the critical pericentric distance for return orbits at which the timescale for two-body relaxation in angular momentum is equal to the timescale for emission of gravitational radiation to shrink and circularize the orbit,

$$R_p^{\rm crit} \sim 10^{12}\,{\rm cm}\left(\frac{a}{10^{18}\,{\rm cm}}\right)^{-1/2} M_6^{5/4} \qquad (12)$$

for a cluster with the assumed stellar mass density profile $\rho(r) \propto r^{-7/4}$ (Bahcall & Wolf 1976). The orbits with pericenters below this critical value will evolve predominantly due to the emission of GWs and those above it will evolve due to the two-body interactions. Note that a large portion of the parameter space outlined in Equation (11) (but not all of it) resides within the GW-dominated regime as long as $a < 10^{18}$ cm. Hence, there is an allowed region of the orbital parameter space where the RG remnant will continue to spiral into the SMBH due to the emission of GWs, such that $10^{15} < a < 10^{18}$ cm and pericenter is in the range given by Equation (11). In the rest of the paper we focus on RG remnants which find themselves on such orbits.

4.2. Evolution Due to the Stripping of the Stellar Envelope

The three-dimensional relativistic hydrodynamic simulations of single encounter between a white dwarf and an intermediate mass black hole by Cheng & Evans (2013) indicate that during partial disruption most of the tidal energy is deposited into the surface layers of the star by shock heating. Radiation can escape the surface layers of the star easier than its denser central parts, which implies that shocks during repeated pericentric passages should cause a characteristic brightening of the RG remnant. As a result, the luminosity, temperature, and timescale for radiation to diffuse out of the surface layers of the star would be similar to those estimated for the fallback of nearly unbound material from the tidal tails in Section 3. In cases when the estimated radiation diffusion timescale ($t_{\rm diff} \approx 7 \times 10^8$ s) is longer than the orbital period of a returning orbit, the rate of tidal heating will be higher than the rate of radiative cooling leading to the net heating of a star. The orbital period of a Keplerian orbit, $2\pi\sqrt{a^3/GM}$, is

$$P_a = 5 \times 10^8\,{\rm s}\,\beta^{-3/2}\left(\frac{1-e}{0.01}\right)^{-3/2} \times \left(\frac{R_*}{10^{12}\,{\rm cm}}\right)^{3/2}\left(\frac{M_*}{1\,M_\odot}\right)^{-1/2}, \qquad (13)$$

and hence $P_a < t_{\rm diff}$ for $e \lesssim 0.99$ orbits around $10^6\,M_\odot$ black holes. The implication of this effect is the increase in luminosity of the stellar remnant as well as the expansion and degeneracy lifting in the outer layers. Because the luminosity of the shocked outer layers of perpetually heated star can become comparable or larger than the stellar Eddington luminosity after only a few orbits (see Equation (7)), the combined effect of radiative pressure and expansion will drive the increased mass-loss of the remainder of the stellar envelope. These two regimes have been previously described in some detail by Alexander & Morris (2003), who studied a class of tidally heated stars called squeezars. Thus, a majority of tidally stripped RG remnants may lose all of their bound hydrogen envelope after several orbital passages by the SMBH. A more precise timescale on which this happens depends on a complex interplay of radiative processes, hydrodynamics, and orbital dynamics and can only be captured though simulations.

We carry out a simple estimate to determine the relative importance of the disruption of the envelope versus the GW

emission for the evolution of the remnant's orbit in the case where the stellar envelope is removed gradually. We assume that the envelope is stripped over N_s orbits, and write the necessary energy budget as

$$\Delta E_s \sim \frac{1}{N_s}\frac{\eta_{\rm env} G M_{\rm core} M_*}{R_*}, \quad (14)$$

where $\eta_{\rm env} = M_{\rm env}/M_*$. We evaluate the energy loss per orbit due to the emission of GWs as

$$\Delta E_{\rm gw} = -\frac{64\pi}{5}\frac{G^{7/2} M^2 M_{\rm core}^2 (M+M_{\rm core})^{1/2}}{c^5 a^{7/2}} f_1(e), \quad (15)$$

where $f_1(e) = (1+73e^2/24+37e^4/96)/(1-e^2)^{7/2}$ (Peters 1964). In the limit when $e \to 1$ this expression becomes

$$\lim_{e\to 1}\Delta E_{\rm gw} = -\frac{85\pi}{12\sqrt{2}}\frac{G^{7/2} M^2 M_{\rm core}^2 (M+M_{\rm core})^{1/2}}{c^5 R_p^{7/2}}. \quad (16)$$

For most orbital parameters considered here the energy loss due to the emission of gravitational radiation is well approximated by the solution based on semi-Keplerian orbits as described in Peters (1964). However, for cores that make very close pericentric passages by the SMBH ($R_p \lesssim 10\, r_g$), this approximation ceases to be accurate. Martell (2004) compared approximations equivalent to the approach by Peters (1964) and more accurate prescriptions and found that the difference in the GW energy loss amounts to a factor between 0.8 and 1.3. This level of approximation is appropriate for our study and we therefore use the Peters approximation.

Combining Equations (14) and (16) in the limit of $e \to 1$ we obtain

$$\frac{\Delta E_s}{\Delta E_{\rm gw}} \sim 3\times 10^4\, \eta_{\rm env}\, \beta^{-7/2} \left(\frac{N_s}{10^4}\right)^{-1} \left(\frac{R_*}{10^{12}\,{\rm cm}}\right)^{5/2} \times \left(\frac{M_*}{1\,M_\odot}\right)^{-1/6} \left(\frac{M_{\rm core}}{0.3\,M_\odot}\right)^{-1} M_6^{-4/3}. \quad (17)$$

Therefore, hydrodynamic effects related to the stripping of the envelope are the dominant driver of the orbital evolution in a majority of scenarios. It is worth noting that if most of the tidal energy (Equation (14)) is absorbed by the core, then repeated tidal interactions can in principle supply a significant fraction of energy necessary to lift the degeneracy of the core. This follows from the energy budget necessary to generate thermal pressure comparable to the degenerate pressure of the core, which can be estimated from the virial theorem of a white dwarf in equilibrium. We consider the tidal heating of the core in more detail in the next section.

It is worth noting that there is an additional mechanism that may drive an increased mass loss from the surface of the star. We do not consider the Roche lobe overflow in this work, but it has been shown by MacLeod et al. (2013) that RG stars on eccentric orbits continue to lose mass from their envelope at each pericentric passage as they overflow the Roche lobe for a short time. For an RG on a relatively stable orbit, the mass loss eventually ceases due to the stabilizing gravitational influence of the compact core.

Recent simulations also indicate that tidal disruption is an inherently asymmetric process and that unequal fractions of the debris are launched toward the SMBH and unbound from the system (Cheng & Evans 2013; Manukian et al. 2013; Kyutoku et al. 2013). This asymmetry is more pronounced (in geometric sense) for the larger mass ratios ($q \gtrsim 10^{-4}$) and arises from the fact that more material escapes from the surface of the star facing the SMBH, relative to the surface that faces away (see Figures 6 and 7 in Cheng & Evans 2013). Since unequal portions of the debris carry unequal amounts of linear momentum, the conservation of linear momentum then requires that the remnant core is deflected from its initial orbit. We neglect this effect which stems from the hydrodynamic interaction of the star with the tides of the SMBH and assume that the core continues to orbit along the geodesic previously occupied by the center of mass of the RG star.

4.3. Tidal Heating of the Core and Emission of Gravitational Waves

In this section, we consider the effect of tidal interaction on the helium core. The SMBH tides drive oscillations which if dissipated within the core lead to a gradual circularization of its orbit. It can be shown that the amount of energy available from circularization is much larger than the gravitational energy of the star (Ivanov & Papaloizou 2007). Namely, the energy released from circularization of an orbit with initial pericentric radius R_p and eccentricity $e \to 1$ is $\Delta E_{\rm circ} \approx GMM_{\rm core}/4R_p$. Comparing that to the gravitational energy of the core, $E_{\rm core} \approx GM_{\rm core}^2/R_{\rm core}$, yields

$$\frac{\Delta E_{\rm circ}}{E_{\rm core}} \approx \frac{1}{4}\beta_{\rm core}\left(\frac{M}{M_{\rm core}}\right)^{2/3} \approx 6\times 10^3 \beta_{\rm core}\left(\frac{M_{\rm core}}{0.3\,M_\odot}\right)^{-2/3} M_6^{2/3}. \quad (18)$$

Even if a small fraction of this energy is deposited into the remnant it is in principle sufficient to lift the degeneracy of the core and possibly dissolve it before the core reaches the tidal radius or plunges into the SMBH (Ivanov & Papaloizou 2007). Recall, however, that at the same time the emission of gravitational radiation is concurrently acting to decrease the orbital eccentricity of the core. If tidal heating is the faster of the two processes, the remnant will be destroyed before the orbit is circularized. If, however, the GW emission is more efficient, the remnant will find itself on a quasi-circular orbit, gradually inspiralling into the SMBH and possibly forming an EMRI (see, for example, Zalamea et al. 2010, who studied mass transfer between an inspiralling white dwarf and a low-mass SMBH in this regime).

To estimate the timescale on which the tides are depositing energy onto the star, we rely on the linear theory of tidal interactions developed for stars and planets on eccentric orbits (Press & Teukolsky 1977; Leconte et al. 2010). The linear theory applies to weak encounters, rather than disruptive ones when description of the tidal interaction as a low level perturbation ceases to be accurate. Consequently, the linear theory can be used to estimate the energy deposited onto a compact core, for which $\beta_{\rm core} \ll 1$, but is not applicable to the stellar envelope that is in the $\beta \gtrsim 1$ regime. In this calculation we therefore consider the tidal heating of the compact core only and do not account for the effects of the envelope (which are discussed in Section 4.2 as an order of magnitude estimate). This is a conservative assumption which leads to a slower orbital evolution of the core since in absence of the envelope $\dot{E}_{\rm tid}$ is only a lower limit on the rate of energy deposition into the remnant. Similar to Amaro-Seoane et al. (2012), we adopt the expression from Leconte

et al. (2010) for the rate at which the orbital energy is lost to the excitation of oscillatory modes within the star

$$\dot{E}_{\rm tid} = 2K_p \left[N_a(e) - \frac{N^2(e)}{\Omega(e)} \right], \tag{19}$$

where the expression in the brackets only depends on eccentricity and can be simplified to $7e^2/2$ for $e < 1$. This is an adequate approximation for the orbital evolution of the helium core, which starts on a highly eccentric orbit and is gradually circularized by tidal heating and GWs. Using their expression for K_p

$$K_p \approx \frac{9}{4} Q^{-1} \left(\frac{G M_{\rm core}^2}{R_{\rm core}} \right) \left(\frac{M}{M_{\rm core}} \right)^2 \left(\frac{R_{\rm core}}{a} \right)^6 \left(\frac{GM}{a^3} \right)^{1/2}. \tag{20}$$

Modifying further to relate a to the orbital pericenter and orbital period, we obtain

$$\dot{E}_{\rm tid} \approx \frac{63\pi}{2} Q^{-1} e^2 \beta_{\rm core}^6 \left(\frac{G M_{\rm core}^2}{R_{\rm core}} \right) P_a^{-1}, \tag{21}$$

where Q is the quality factor, a parameterization of the coupling of the tidal field to the stellar core. The magnitude of Q is quite uncertain and commonly assumed in the literature to be in the range $\sim 10^5$–10^6. However, a recent work by Prodan & Murray (2012) indicates that the quality factor of helium white dwarfs may be even higher (they find $Q \gtrsim 10^7$) but these types of measurements are complicated by the fact that the value of Q can only be determined as a lower limit and is coupled to other (uncertain) parameters of the system.

We calculate the characteristic time for circularization of the RG core orbit assuming that tidal dissipation within the remnant is efficient and obtain

$$\tau_{\rm tid} = \frac{\Delta E_{\rm circ}}{\dot{E}_{\rm tid}} = \frac{1}{126\pi} \frac{Q}{\beta_{\rm core}^6 e^2} \left(\frac{M}{M_{\rm core}} \right)^{2/3} P_a. \tag{22}$$

We then calculate the amount of time it takes to circularize the orbit due to the emission of GWs (Peters 1964)

$$\tau_{\rm gw} = \frac{e}{\dot{e}} = \frac{15}{608\pi} f_2(e) \beta_{\rm core}^{-5/2} \left(\frac{R_{\rm core}}{r_g} \right)^{5/2} \left(\frac{M}{M_{\rm core}} \right)^{11/6} P_a, \tag{23}$$

where $f_2(e) = (1 + 121e^2/304)^{-1}$. Comparing the two timescales yields

$$\frac{\tau_{\rm tid}}{\tau_{\rm gw}} \approx 2 \times 10^3 \frac{\beta_{\rm core}^{-7/2}}{e^2 f_2(e)} Q_6 \left(\frac{R_{\rm core}}{10^9\,{\rm cm}} \right)^{-5/2} \left(\frac{M_{\rm core}}{0.3\,M_\odot} \right)^{7/6} M_6^{4/3}, \tag{24}$$

where $10^6 Q_6 = Q$. Hence, the gravitational radiation will always circularize the core's orbit on a timescale much shorter than that for the tidal circularization. This implies that only a fraction of the energy available from orbital circularization will be deposited into the remnant. How large that fraction is in terms of the remnant's binding energy depends on the properties of the core, its orbit, and the mass of the black hole. Equations (18) and (24), for example, indicate that close to disruption ($\beta_{\rm core} \sim 1$), the core can in principle absorb $\sim 6 \times 10^3/2 \times 10^3 \sim$ few times its binding energy by the time its orbit is circularized due to the emission of GWs. However, the compact core considered here reaches the maximum penetration factor, $\beta_{\rm core}^{\rm max} \approx 0.5 < 1$ at the event horizon of a $10^6\,M_\odot$ SMBH,

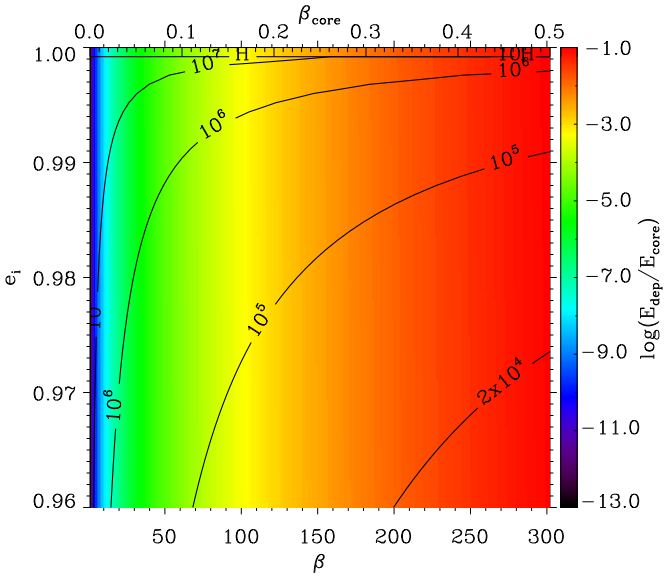

Figure 1. Color illustrates the maximum tidal energy deposited into the inspiralling stellar core (in units of its binding energy) as a function of the initial orbital eccentricity (e_i) and strength of the tidal encounter (β). The top axis shows the corresponding penetration factor for the core alone. Black solid lines mark the orbital period of the core in seconds. Orbits in the top part of the figure have periods longer than the Hubble time, as marked by the letter "H."

(A color version of this figure is available in the online journal.)

where the amount of energy deposited into it is at maximum $\sim 0.08 E_{\rm core}$.

This is illustrated in Figure 1 where the color bar shows the maximum tidal energy deposited into the inspiralling stellar core as a function of the initial orbital eccentricity (e_i) and strength of the tidal encounter (β and $\beta_{\rm core}$). This energy will be stored within the core because it is deposited on a timescale shorter than that on which it can be radiated (i.e., the Kelvin–Helmholtz timescale). Since $\tau_{\rm KH} = E/L$ (where E is the thermal energy of the white dwarf-like core) the more luminous cores tend to cool faster. Indeed, theoretical calculations of white dwarf cooling sequences show that a $0.3\,M_\odot$ white dwarf with luminosity between $0.3 > L > 10^{-4}\,L_\odot$ cools on a timescale $10^8 < \tau_{\rm KH} < 10^{10}$ yr, respectively (Driebe et al. 1998; Nelemans et al. 2001). For the cores with a representative cooling timescale of $\tau_{\rm KH} \sim 10^9$ yr $\gg \tau_{\rm gw}$, the evolution may proceed similar to squeezars, tidally powered stars that find themselves on non-disruptive orbits (Alexander & Morris 2003).

4.4. Interaction of the Core with the Envelope Debris Disk

We now consider the interaction of the RG remnant on a return orbit with the accretion disk that forms from the tidally stripped hydrogen stellar envelope. By the time the core returns, the inner parts of the debris disk have had time to complete multiple orbits and start circularizing (Ulmer 1999). As a consequence, the debris is more spatially extended than the core's orbit at separation $\sim R_T$ from the SMBH leading to the intersection of their orbits. Based on considerations in Section 2 we estimate that a core encounters the debris disk with radius $\sim 2R_T$ and mass in the range $M_{\rm disk} \approx 0.2$–$0.7\,M_\odot$, where the lower bound corresponds to parabolic encounters at the threshold of disruption and the upper bound corresponds to $\beta > 1$ encounters where the RG star is initially placed on moderately eccentric, bound orbit.

The core can only experience significant orbital energy losses if it encounters the amount of disk mass comparable to its own. Since the debris disk is spread to a very low density, the remnant will not be able to sweep a mass equivalent to its own even after many passages and thus, the effect of the disk on the orbit of the remnant can be neglected. This outcome is guaranteed given a relatively short estimated timescale for accretion of the debris, $t_{\rm acc} \sim$ few $\times\ P_{\rm m}$ (see Section 3), indicating that the debris disk will be accreted and dispersed before it can impact the RG core in any way.

Along similar lines, given a relatively short lifetime of the transient disk, it is also unlikely that the core-disk collisions can give rise to more than a few quasi-periodic luminosity outbursts.

5. TIDAL DISRUPTION CANDIDATE PS1-10jh

5.1. Constraints on the Properties of the RG Remnant

We now consider a recently discovered tidal disruption candidate PS1-10jh described by Gezari et al. (2012). PS1-10jh was discovered as an optical transient in the Pan-STARRS1 Medium Deep Survey and independently as a near-ultraviolet source within the *GALEX* Time Domain Survey. Based on the modeling of the multi-band photometry and optical spectra of this object, Gezari et al. (2012) proposed that the disrupted object is a tidally stripped helium core of an RG star that initially had mass $M_* \gtrsim 1\ M_\odot$. They adopt properties of the core consistent with those measured for an RG stellar remnant stripped in a stellar binary system (Maxted et al. 2011), where $M_{\rm core} \sim 0.23\ M_\odot$ and $R_{\rm core} \sim 0.33\ R_\odot$, and use the local scaling relations and tidal disruption light curve to constrain the mass of the SMBH to $M \approx 2.8 \times 10^6\ M_\odot$.

Note that the radius of the remnant adopted by Gezari et al. (2012) is an order of magnitude larger than that of the "bare" helium core we consider in previous sections (based on models of Hamada & Salpeter 1961; Althaus & Benvenuto 1997). This is because a low-mass RG remnant created through stripping and mass transfer in a stellar binary is expected to retain some fraction of its hydrogen envelope in which hydrogen burning is maintained in a shell. The luminosity contribution due to the nuclear burning drives the expansion of the envelope and degeneracy lifting in the exterior shells of such white dwarf and results in the radius of the remnant typically a few times larger than that of a pure helium core (Driebe et al. 1998, 1999).

The choice of the RG remnant structure has important implications for the outcome of the tidal interaction. Specifically, a bare helium core considered previously is too compact in size to be disrupted by the SMBH (Figure 1), while the core with the radius $\approx 0.33\ R_\odot$ considered by Gezari et al. (2012) can be disrupted after multiple passages (this will be shown in the next section). What is a more realistic choice for the structure of the remnant is a question of some subtlety. Even if the RG core initially had a radius of $\sim 10^9$ cm, given a sudden loss of 30%–50% of the RG mass during its first pericentric passage (see Section 2), the core will have to adjust to a new equilibrium by expanding beyond its original radius. We estimate the change in the radius of the core from the mass–radius relation for the adiabatic evolution of a nested polytrope, as outlined by MacLeod et al. (2013). Depending on the adopted value of the polytropic index, one finds that the new radius of the remnant can be up to 5.5 times larger.[8] Therefore, we expect that the radius of the remnant core in the case of PS1-10jh to be larger than that of the core in an intact RG and for the purpose of the analysis in this section adopt the mass and radius suggested by Gezari et al. (2012).

Several observational properties of PS1-10jh offer important clues about the remnant.

1. The temporal decay of the light curve closely follows the canonical prediction $L_{\rm fb} \propto t^{-5/3}$ indicating that the incoming core must have been on a highly eccentric orbit prior to disruption such that at least one portion of it ended up being gravitationally unbound from the system. It has otherwise been shown that lower eccentricity encounters in which 100% of the debris is gravitationally bound to the black hole have the fallback accretion rate significantly different from $\propto t^{-5/3}$ (Hayasaki et al. 2013; Dai et al. 2013, see however the end of this section for further discussion of this point).
2. An interesting property of PS1-10jh are its broad high-ionization He II lines (with wavelengths $\lambda = 4686$ Å and $\lambda = 3203$ Å) which are contrasted by the absence of the hydrogen emissions lines. Gezari et al. (2012) find that the lack of hydrogen Balmer lines requires a very low hydrogen mass fraction of <0.2, thus supporting the picture that the disrupted star is a helium core. The lack of any emission lines from the hydrogen stellar envelope, which is expected to be several times more massive than the core in the progenitor RG star, is, however, puzzling and is the key to understanding the nature of this event.
3. The characteristic temperature of the emitted radiation from PS1-10jh has remained relatively uniform before and after the disruption ($T \gtrsim 3 \times 10^4$ K). The lack of evolution of the spectrum indicates that the observed radiation may have been reprocessed by the obscuring layer or a shell, enshrouding the inner debris disk. Because the luminosity for this system can only be determined as a lower limit, $\gtrsim 0.6\ L_{\rm Edd}$ (Gezari et al. 2012), it follows that both the radiation forces and relativistic frame-dragging are viable candidates for a mechanism that can distribute the debris across the sky and create obscuration.

The expectation that the fallback accretion rate differs significantly from $\propto t^{-5/3}$ for disruption of stars on initially bound orbits with moderate eccentricities ($e \lesssim 0.99$) is based on theoretical studies by Dai et al. (2013) and Hayasaki et al. (2013), who carried out the particle and hydrodynamic simulations of this scenario, respectively. There is, however, an inherent uncertainty in interpretation of simulated accretion rates in terms of the observed tidal disruption light curves, since these simulations do not account for the effects of radiative feedback nor do they model accretion light curves in a given wavelength band. We acknowledge this uncertainty in the step where we suggest that an observed optical light curve of PS1-10jh with behavior close to $L_{\rm fb} \propto t^{-5/3}$ indicates a similar power-law behavior in the underlying accretion rate.

5.2. Disruption of the Envelope and Inspiral of the Compact Core

One possible explanation for the absence of hydrogen emission lines is that most of the tidally stripped envelope was accreted by the black hole before the helium core disruption (see the next subsection for discussion about other possible explanations). This scenario could play out if the RG core completed multiple orbits before being disrupted by the SMBH during

[8] See also MacLeod et al. (2013) for a discussion of why the response of the remnant in reality may be different and potentially more dramatic than indicated by the polytropic model.

which time the envelope was nearly completely stripped and accreted. We consider the orbital properties of the incoming RG star which could have given rise to such a sequence of events and can simultaneously satisfy the described observational properties. A condition for partial disruption which must be satisfied in order to have the RG envelope stripped by the tidal forces and the compact core intact is $\beta \geqslant 1$ and $\beta_{\rm core} < 1$. We assume that the stellar core had a relatively common RG progenitor star with mass and radius $M_* = 1.4\,M_\odot$ and $R_* = 10^{12}$ cm. Note that these choices are uncertain even though they are physically motivated, as the evolutionary sequence of the helium remnant cannot be constrained more precisely from the available data. Based on this adopted structure and Equation (3), we find that the penetration factor of the compact core is $\beta_{\rm core} \approx \beta/24$ and thus there is a range in β-parameter space for which partial disruption can be achieved.

In order for most of the hydrogen envelope to be accreted, it must be placed on bound eccentric orbits around the SMBH. It is possible to estimate from analytic arguments the critical orbital eccentricity below which the entire envelope is bound. From the condition that the orbital energy of the RG envelope (and the star) is equal to the energy spread in the tidal field of the black hole at the point on the orbit when the envelope is removed we find

$$\frac{GM(1-e)}{2R_p} = \frac{GM\,R_*}{R_T^2}. \quad (25)$$

From this condition, it follows that the initial eccentricity of the RG stellar orbit must be smaller than $e_{\rm crit}^{\rm env} \approx 1 - (2/\beta)(M_*/M)^{1/3}$ in order for the entire envelope to be bound to the SMBH (Hayasaki et al. 2013). We derive a similar condition for the first pericentric passage of the RG core,

$$\frac{GM(1-e)}{2R_p} = \frac{GM\,R_{\rm core}}{R_p^2}. \quad (26)$$

Note that in this case the spread in energy reaches maximum at the pericenter of the orbit, rather than at the tidal radius of the envelope and that $R_p = R_T/\beta = R_T^{\rm core}/\beta_{\rm core}$. This implies a critical eccentricity value of $e_{\rm crit}^{\rm core} \approx 1 - (2\beta_{\rm core})(M_{\rm core}/M)^{1/3}$ and is valid when $\beta_{\rm core} < 1$.

The $\propto t^{-5/3}$ temporal behavior of the disruption light curve indicates that at least one portion of the tidally disrupted core is not bound to the SMBH. It follows that the eccentricity of the first orbit of the RG star must satisfy the condition $e_{\rm crit}^{\rm core} < e_i < e_{\rm crit}^{\rm env}$. This criterion is satisfied only when $e_{\rm crit}^{\rm core} < e_{\rm crit}^{\rm env}$ leading to

$$\beta\beta_{\rm core} > \left(\frac{M_*}{M_{\rm core}}\right)^{1/3} \quad (27)$$

and, consequently, $6 < \beta < 24$, or written in terms of the core penetration factor, $0.25 < \beta_{\rm core} < 1$. Hence, there is a portion of the parameter space conducive to disruption of the RG envelope followed by the disruption of the core upon completion of some number of orbits by the core. In such a case, the hydrogen envelope ends up bound to the SMBH in its entirety, while the debris created by the subsequent disruption of the helium core is only partially bound. It is important to point out that the exact bounds within which this region lies are approximate, as they are derived from simple analytic considerations. However, a realization that such a region must exist for highly eccentric orbits, naturally follows from the difference in the relative spread in energies of the core and envelope.

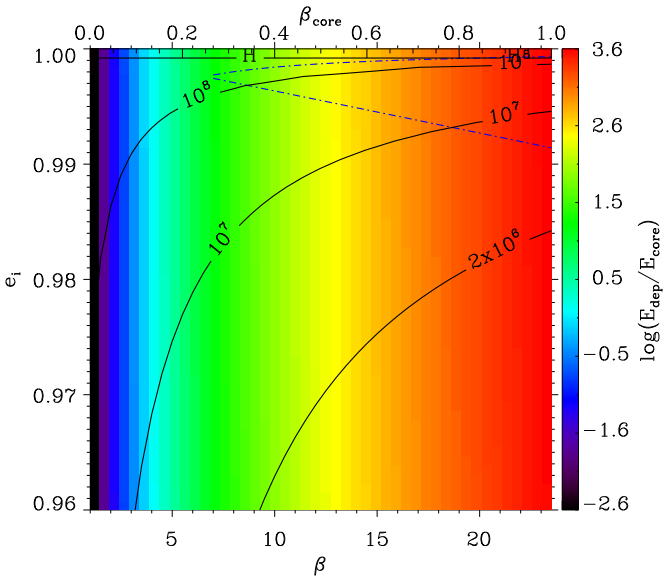

Figure 2. Similar to Figure 1, except that color here illustrates the maximum tidal energy deposited into the inspiralling stellar core in PS1-10jh. Blue dash–dotted line marks the region where RG star is partially disrupted and its hydrogen envelope can be accreted before the disruption of the compact core.

(A color version of this figure is available in the online journal.)

The inspiralling core will be subject to tidal heating and emission of gravitational radiation, as discussed in Section 4.3. Taking the ratio of Equations (18) and (24), we calculate the maximum tidal energy that can in principle be deposited into the remnant before gravitational radiation circularizes its orbit. For the assumed mass and radius of the helium core disrupted in PS1-10jh and the inferred mass of the SMBH we find

$$\frac{E_{\rm dep}}{E_{\rm core}} \sim 5\times10^3\,e^2\,f_2(e)\,Q_6^{-1}\beta_{\rm core}^{9/2}\,M_{\rm core}^{-11/6}\,R_{\rm core}^{5/2}\,M^{-2/3}, \quad (28)$$

where $M_{\rm core}$, $R_{\rm core}$, and M have been normalized to the appropriate values for this system. The amount of the deposited tidal energy is a strong function of $\beta_{\rm core}$. Given that we are considering the $\beta_{\rm core} < 1$ portion of the parameter space, where the core gradually inspirals into the SMBH, the ratio of $E_{\rm dep}/E_{\rm core}$ will generally be lower than the estimate in Equation (28).

In Figure 2 the color bar shows the maximum tidal energy deposited into the inspiralling stellar core as a function of the initial orbital eccentricity (e_i) and strength of the tidal encounter (β and $\beta_{\rm core}$). In this parameter space $\beta_{\rm core} > 0.2$ encounters can in principle deposit the amount of tidal energy larger than $E_{\rm core}$ prior to orbital circularization and thus lift the degeneracy of the core and lead to its disruption before it reaches the tidal radius (note that this is different from the outcome shown in Figure 1). This can be accomplished as long as the tidal energy is stored in the core over many orbits and not efficiently radiated. The initial orbital period of the core is shown in seconds as a function of e_i and $\beta_{\rm core}$ with black contour lines. This indicates that the majority of this parameter space comprises of initial orbital periods $<\tau_{\rm KH}$. The portion of the parameter space where $e \approx 1$ is characterized by orbital periods longer than the Hubble time is indicated by the letter "H."

In Figure 2 we also mark the region within which the criterion for partial disruption described by Equation (27) is satisfied (blue dash–dotted line). The region is confined to a narrow strip of high eccentricities with values $e > 0.991$, characteristic of stellar objects that fall toward the black hole on a nearly

parabolic orbit. The incoming RG star must occupy the region below the upper dash–dotted line in order for its hydrogen envelope to be entirely bound to the SMBH after it is stripped. The observed temporal behavior of the light curve in PS1-10jh on the other hand indicates that at the point of disruption the helium remnant must still have occupied a very eccentric orbit, somewhere above the lower dash–dotted line. This region is characterized by orbits with the period in the range $\sim 10^7$–10^8 s, GW circularization times in the range $\sim 10^7$–10^9 yr, and intense tidal interaction with maximum deposited tidal energy in the range ~ 10–$5 \times 10^3 E_{\rm core}$. The core occupying this portion of the parameter space would therefore have had time to complete many of orbits before the deposited tidal energy is radiated on a Kelvin–Helmholtz timescale. It is thus likely that such a core would have its degeneracy lifted by perpetual episodes of tidal heating, leading to premature disruption. An early disruption would also ensure that the core remains on a highly eccentric orbit, before the GW emission had time to circularize it significantly.

The observed light curve of PS1-10jh also indicates that the white dwarf-like core would have to undergo a single disruption event at the end of the tidal heating period, rather than produce a series of quasi-periodic accretion events as the core overflows its Roche lobe at every pericentric passage. The latter scenario has been modeled by Zalamea et al. (2010), who find that the resulting accretion curve consists of multiple exponentiating flares very distinct from the $\dot{M} \propto t^{-5/3}$ behavior. We propose that the core undergoes a single disruption scenario if the imparted tidal energy can be redistributed over the volume of the remnant, maintaining the evolution through a series of quasi-equilibria and avoiding rapid expansion of the outer layers and stripping.

The timescale on which the tidal energy can be transported from the surface of the remnant inward is given by its thermal diffusion timescale, $\tau_{\rm cond} = R_{\rm core}^2/\chi_{\rm th} \sim 10^6$ yr, where $\chi_{\rm th}$ is the diffusivity constant (Padmanabhan 2001). The hierarchy of timescales $P_a \ll \tau_{\rm cond} \ll \tau_{\rm KH}$ implies that tidal interactions establish a temperature gradient between the surface and the center of the remnant that last over many orbits but that the tidal energy is diffused throughout it before the remnant has a chance to cool radiatively. It is thus plausible in this regime to tidally heat the remnant gradually, although some amount of tidal stripping from the surface of the remnant is likely at the rate lower than that found by Zalamea et al. (2010).

5.3. "Disappearance" of the Hydrogen Envelope

In the mean time, the stripped stellar envelope forms an accretion disk with maximum initial mass $M_{\rm disk,i} = M_* - M_{\rm core} \approx 1.2\,M_\odot$, which circularizes and accretes onto the SMBH. The observations of PS1-10jh indicate that at the moment of disruption of the helium core the mass fraction of hydrogen must have been more than five times lower relative to helium and other atomic species thus, placing the upper limit on the final mass of the hydrogen disk to $M_{\rm disk,f} < 0.2 M_{\rm core} \approx 0.05\,M_\odot$. Integrating over the accretion rate in Equation (5), we find that this portion of the disk would be accreted after $t_{\rm acc} \sim P_{\rm m}$. For the parameters considered here, the orbital period of the debris deepest in the SMBH potential well is $P_{\rm m} \sim 2 \times 10^8$ s and is shorter for more bound configurations of the envelope, corresponding to RG orbits with lower initial eccentricity. This implies that with a moderate or low level radiative feedback the gas would be swallowed by the black hole on a timescale ~ 10 yr. Alternatively, strong radiative feedback would promptly disperse and ionize the debris. This timescale places a lower limit constraint on the time between the disruption of the hydrogen envelope and disruption of the helium core. Note that PS1-10jh was not detected in 2009 in the deep coadd of the *GALEX* time domain survey with a $\sim 3\sigma$ upper limit of >25.6 mag (Gezari et al. 2012). In the context of our model this indicates that by that point most of the disk must have been accreted or dispersed.

Another possible explanation for the weakness or absence of the hydrogen emission lines is that the debris hydrogen envelope may be present at the disruption site in the vicinity of the SMBH, but is completely ionized or produces a negligible amount of hydrogen emission. Tidal disruptions have indeed been proposed to create a highly ionized nebular emission from the ISM in the inner kiloparsec of their host galaxies (Eracleous et al. 1995). This scenario is considered by Guillochon et al. (2014), where three-dimensional hydrodynamic simulations show the disruption of a low mass main sequence star ($\sim 0.2\,M_\odot$) with debris forming a finite size BLR, truncated at the outer radius. The compact BLR consists of gas from the disrupted star including hydrogen, but effectively behaves as an H II region and consequently emits weak hydrogen emission lines below the current detection threshold. He II emission-line on the other hand remains present in the spectrum longer due to the higher ionization potential of this element. In this scenario, the unbound tidal stream has a negligible surface area and makes negligible contribution to either the continuum or line emission. This explanation is consistent with the finding that the luminosity of the hydrogen Balmer lines from the tidal disruption of a solar type star by a $10^6\,M_\odot$ SMBH is $\lesssim 10^{39}\,{\rm erg\,s^{-1}}$ (Bogdanović et al. 2004), and thus, below the detection threshold of the available spectroscopic data for PS1-10jh. This work, however, does not address the intensity of the helium emission-lines and hence does not constrain the He/H line ratio. Recently, Gaskell & Rojas Lobos (2014) carried out the one-dimensional photoionization modeling of the emission properties of gas in truncated BLRs[9] and concluded that strong helium emission does not require depletion of hydrogen. Specifically, they find that the He II $\lambda 4686/{\rm H}\alpha$ line ratio peaks at the value as high as ~ 4.0 when the gas density is $\sim 10^{11}\,{\rm cm^{-3}}$, given a solar abundance ratio of the two elements. This line ratio is a sensitive function of the gas density, however, and the work by Gaskell & Rojas Lobos (2014) also indicates that unless most of the solar metallicity debris resides in the density range $10^{10} < n < 10^{12}\,{\rm cm^{-3}}$, the value of the line ratio He II $\lambda 4686/{\rm H}\alpha \lesssim 1$. Stellar debris produced in tidal disruptions is indeed characterized by a wide range of densities and is spatially distributed over eccentric orbits, allowing multiple density phases of gas to reside at the same distance from the ionization source (Bogdanović et al. 2004; Strubbe & Quataert 2009, 2011). The non-axisymmetric distribution of the gas results in a more complex emission stratification than in the BLR regions of AGN that does not a priory preclude the emission of the broad hydrogen lines. Indeed, more recent and detailed calculations indicate that it is difficult to suppress them to the level consistent with the observed properties of PS1-10jh (L. E. Strubbe & N. Murray 2014, in preparation).

Given the difficulty to "hide" the hydrogen emission lines in the presence of the illuminated hydrogen rich stellar debris, in this work we consider a family of models that lead to a

[9] In this approach, the photoionization properties of the gas are calculated as a function of distance from the ionization source.

near complete accretion rather than dispersal, of the hydrogen envelope of the partially disrupted RG star. In the context of this hypothesis, at a later point in time when the helium core is disrupted, helium dominates the optical emission line spectrum, as predicted by the photoionization calculations of the spectrum from a tidally disrupted white dwarf by Sesana et al. (2008). This is also consistent with the work Clausen & Eracleous (2011), who find that the UV and optical spectrum of a tidally disrupted carbon–oxygen white dwarf is dominated by these species and characterized by the overall lack of hydrogen emission lines. It is also worth noting that have the multiple and more varied emission line features been seen in the spectrum of PS1-10jh, it would be possible to put stronger constrains on the structure of the disrupted RG star and the mass of the black hole. This is illustrated by Clausen et al. (2012) who found a good agreement of their modeled emission line spectrum from the disruption of a horizontal branch star by a BH with that observed from the globular cluster NGC 1399 which hosts the ultraluminous X-ray source CXOJ033831.8-352604.

5.4. Distribution of the Helium-rich Debris on the Sky

The favored portion of the parameter space, $6 < \beta < 24$ marked in Figure 2, maps into pericentric radii in the range $\sim$13–52 r_g. At this distance the helium core and its debris are subject to relativistic effects such as pericenter precession (see Guillochon et al. 2014, for discussion of this effect) and precession of the orbital plane, if the orbital axis and spin of the SMBH are misaligned.

Evidence that relativistic effects can lead to the extended distribution of the debris can be found in work by Haas et al. (2012), who simulated the disruption of a white dwarf star by a spinning IMBH with arbitrarily oriented spin axes. They find that as a consequence of frame-dragging, the stellar debris forms an optically and geometrically thick torus rather than an accretion disk. This leads to the obscuration of the inner fallback disk by the outflowing debris. As a consequence, the spectrum from the debris is softer because it is mostly emitted by the material further away from the black hole. Along similar lines, Loeb & Ulmer (1997) have calculated the temperature of radiation reprocessed and re-emitted at the Eddington limit by an optically thick, static shell of gas with mass $\sim 0.1\,M_\odot$ enshrouding the inner debris accretion disk

$$T_{\rm shell} \approx \left(\frac{L_E}{4\pi R_{\rm out}^2 \sigma}\right)^{1/4} = 2.5\times 10^4\,{\rm K}\left(\frac{M}{10^7 M_{\rm env}}\right)^{1/4}, \quad (29)$$

where $R_{\rm out}$ is defined as the photospheric radius—the radius at which the optical depth to Thomson scattering $\tau_T = 1$. $T_{\rm shell}$ calculated in Equation (29) is comparable to the characteristic temperature of radiation maintained by PS1-10jh throughout the disruption. This finding, combined with the fact that the range for the peak bolometric luminosity of PS1-10jh inferred from observations permits values lower than the Eddington luminosity (Gezari et al. 2012), leaves room for relativistic effects as a plausible explanation for the configuration and emission properties of the debris in PS1-10jh.

6. CONCLUSIONS

We consider the tidal interaction of an RG star with an SMBH in which the disruption is partial, leading to the tidal stripping of the star's hydrogen envelope and subsequent inspiral of the compact helium core toward the black hole. Depending on its structure and the SMBH mass, the helium core could either inspiral until it falls into the SMBH or be tidally disrupted, giving rise to a second disruption flare following the disruption of the hydrogen envelope.

During the phase in which the RG envelope is stripped, the orbital evolution of the remnant is determined by tidal interaction which dominates over the emission of GWs. The details of this process are uncertain, cannot be evaluated analytically, and require three-dimensional hydrodynamic simulations to determine the dynamics of the compact core. This deserves further attention because some fraction of the remnant cores will evolve to become EMRIs detectable by the future space-based GW observatories. The envelope effects operating on these types of EMRIs can drive the frequency evolution of their GWs and consequently determine how quickly they "migrate" into or out of the frequency band of the detector, thus affecting their observability and potentially providing a key feature for their identification.

Once the envelope is lost a pure helium core is not easily flexed by the SMBH's tidal field and from that point on the emission of gravitational radiation dominates the orbital evolution and tidal dissipation plays a secondary role. Since the Kelvin–Helmoltz timescale of helium white dwarfs is long ($\sim 10^9$ yr), a significant fraction of the dissipated energy can be retained within the RG remnant. Whether or not perpetual tidal heating episodes lead to the disruption of the remnant depends on its structure, as well as the initial orbit and the SMBH mass. For example, we find that for compact remnants with $M_{\rm core} = 0.3\,M_\odot$ and $R_{\rm core} = 10^9$ cm the deposited energy is only a small fraction of their binding energy and such surviving cores are possible progenitors of EMRIs. On the other hand, less massive and compact cores orbiting around $\sim 10^6\,M_\odot$ SMBHs can be destroyed by tidal heating and hence, they form a parent population for tidally disrupted cores.

In the case of a recently discovered tidal disruption candidate PS1-10jh, we find that there is a set of orbital solutions at high eccentricities, consistent with a nearly parabolic initial orbit of the RG star, which lead to the accretion of the tidally stripped hydrogen envelope by the SMBH before the inspiralling helium core is disrupted. The allowed solutions confine the remnant to a portion of the parameter space where tidal heating is intense and can result in disruption of the core before it reaches the tidal radius. In this scenario, the hydrogen envelope ends up bound to the SMBH in its entirety and is accreted on the timescale of about 10 yr, placing a lower limit on the time between the disruption of the hydrogen envelope and disruption of the helium core. On the other hand, the helium debris produced by the subsequent disruption of the RG core on a highly eccentric orbit is only partially bound, thus giving rise to the canonical power-law decay of the late luminosity curve observed in PS1-10jh. This sequence of events can provide one plausible explanation for the puzzling absence of the hydrogen emission lines from the spectrum of PS1-10jh, interpreted as an apparent absence of the hydrogen envelope at the point in time when the core is disrupted.

Furthermore, the indication that the UV and soft X-ray radiation emitted from the nuclear debris disk is reprocessed by an intervening shell of helium debris can be explained if one portion of the debris assumes a geometrically extended, torus-like geometry around the black hole. In the case of PS1-10jh the leading culprit responsible for this configuration of the debris are radiation forces but also the relativistic frame dragging due to the spinning SMBH. If so, it is intriguing to consider whether

the light curve and spectrum of PS1-10jh may contain any other imprints of the SMBH spin. In order to provide an answer to that question, we need a more systematic understanding of the dependance of the disruption signatures on the black hole spin, which can be achieved through simulations of these events.

The wide-field and high-cadence transient surveys such as *GALEX*, Pan-STARRS, Palomar Transient Factory, and the Large Synoptic Survey Telescope, are expected to detect many more tidal disruption events over the next decade. Therefore, the development of a new generation of theoretical models is timely, as increasingly diverse tidal disruption events are being captured in observations.

T.B. thanks Michael Eracleous, Suvi Gezari, Pablo Laguna, Linda Strubbe, and Fabio Antonini for insightful comments and Lars Bildsten for useful discussion about the properties of the ELM WDs. T.B. acknowledges the support from the Alfred P. Sloan Foundation under grant No. BR2013-016. P.A.S. acknowledges support from the Transregio 7 "Gravitational Wave Astronomy" financed by the Deutsche Forschungsgemeinschaft DFG (German Research Foundation). This research was supported in part by the National Science Foundation under grant No. NSF PHY-1125915 and NSF AST-1333360. The authors acknowledge the hospitality of the Kavli Institute for Theoretical Physics where one part of this work has been completed.

REFERENCES

Alexander, T., & Morris, M. 2003, ApJL, 590, L25
Althaus, L. G., & Benvenuto, O. G. 1997, ApJ, 477, 313
Amaro-Seoane, P., Aoudia, S., Babak, S., et al. 2013a, GW Notes, 6, 4
Amaro-Seoane, P., Miller, M. C., & Kennedy, G. F. 2012, MNRAS, 425, 2401
Amaro-Seoane, P., Sopuerta, C. F., & Freitag, M. D. 2013b, MNRAS, 429, 3155
Bade, N., Komossa, S., & Dahlem, M. 1996, A&A, 309, L35
Bahcall, J. N., & Wolf, R. A. 1976, ApJ, 209, 214
Bogdanović, T., Eracleous, M., Mahadevan, S., Sigurdsson, S., & Laguna, P. 2004, ApJ, 610, 707
Brem, P., Amaro-Seoane, P., & Sopuerta, C. F. 2014, MNRAS, 437, 1259
Carter, B., & Luminet, J. P. 1982, Natur, 296, 211
Chandrasekhar, S., & Bok, B. J. 1942, Sci, 96, 160
Cheng, R. M., & Evans, C. R. 2013, PhRvD, 87, 104010
Clausen, D., & Eracleous, M. 2011, ApJ, 726, 34
Clausen, D., Sigurdsson, S., Eracleous, M., & Irwin, J. A. 2012, MNRAS, 424, 1268
Dai, L., Escala, A., & Coppi, P. 2013, ApJL, 775, L9
Dale, J. E., Davies, M. B., Church, R. P., & Freitag, M. 2009, MNRAS, 393, 1016
Davies, M. B., Church, R. P., Malmberg, D., et al. 2011, in ASP Conf. Proc., The Galactic Center: A Window to the Nuclear Environment of Disk Galaxies, Vol. 439, ed. M. R. Morris, Q. D. Wang, & F. Yuan (San Francisco, CA: ASP), 212
Donley, J. L., Brandt, W. N., Eracleous, M., & Boller, T. 2002, AJ, 124, 1308
Driebe, T., Blöcker, T., Schönberner, D., & Herwig, F. 1999, A&A, 350, 89
Driebe, T., Schoenberner, D., Bloecker, T., & Herwig, F. 1998, A&A, 339, 123
Eracleous, M., Livio, M., & Binette, L. 1995, ApJL, 445, L1
Evans, C. R., & Kochanek, C. S. 1989, ApJL, 346, L13
Frank, J., King, A., & Raine, D. J. 2002, Accretion Power in Astrophysics (Cambridge: Cambridge Univ. Press), 398
Frank, J., & Rees, M. J. 1976, MNRAS, 176, 633
Gaskell, C. M., & Rojas Lobos, P. A. 2014, MNRAS, 438, L36
Gezari, S., Basa, S., Martin, D. C., et al. 2008, ApJ, 676, 944
Gezari, S., Chornock, R., Rest, A., et al. 2012, Natur, 485, 217
Gezari, S., Heckman, T., Cenko, S. B., et al. 2009, ApJ, 698, 1367
Gezari, S., Martin, D. C., Milliard, B., et al. 2006, ApJL, 653, L25
Gomboc, A., & Čadež, A. 2005, ApJ, 625, 278
Greiner, J., Schwarz, R., Zharikov, S., & Orio, M. 2000, A&A, 362, L25
Grupe, D., Beuerman, K., Mannheim, K., et al. 1995a, A&A, 300, L21
Grupe, D., Beuermann, K., Mannheim, K., et al. 1995b, A&A, 299, L5
Grupe, D., Thomas, H.-C., & Leighly, K. M. 1999, A&A, 350, L31
Guillochon, J., Manukian, H., & Ramirez-Ruiz, E. 2014, ApJ, 783, 23
Guillochon, J., & Ramirez-Ruiz, E. 2013, ApJ, 767, 25
Haas, R., Shcherbakov, R. V., Bode, T., & Laguna, P. 2012, ApJ, 749, 117
Hamada, T., & Salpeter, E. E. 1961, ApJ, 134, 683
Hayasaki, K., Stone, N., & Loeb, A. 2013, MNRAS, 434, 909
Ivanov, P. B., & Papaloizou, J. C. B. 2007, A&A, 476, 121
Kesden, M. 2012a, PhRvD, 85, 024037
Kesden, M. 2012b, PhRvD, 86, 064026
Kobayashi, S., Laguna, P., Phinney, E. S., & Mészáros, P. 2004, ApJ, 615, 855
Komossa, S., & Greiner, J. 1999, A&A, 349, L45
Komossa, S., Halpern, J., Schartel, N., et al. 2004, ApJL, 603, L17
Kyutoku, K., Ioka, K., & Shibata, M. 2013, PhRvD, 88, 041503
Lacy, J. H., Townes, C. H., & Hollenbach, D. J. 1982, ApJ, 262, 120
Leconte, J., Chabrier, G., Baraffe, I., & Levrard, B. 2010, A&A, 516, A64
Li, L.-X., Narayan, R., & Menou, K. 2002, ApJ, 576, 753
Lodato, G., King, A. R., & Pringle, J. E. 2009, MNRAS, 392, 332
Lodato, G., & Rossi, E. M. 2011, MNRAS, 410, 359
Loeb, A., & Ulmer, A. 1997, ApJ, 489, 573
MacLeod, M., Guillochon, J., & Ramirez-Ruiz, E. 2012, ApJ, 757, 134
MacLeod, M., Ramirez-Ruiz, E., Grady, S., & Guillochon, J. 2013, ApJ, 777, 133
Magorrian, J., & Tremaine, S. 1999, MNRAS, 309, 447
Manukian, H., Guillochon, J., Ramirez-Ruiz, E., & O'Leary, R. M. 2013, ApJL, 771, L28
Martel, K. 2004, PhRvD, 69, 044025
Maxted, P. F. L., Anderson, D. R., Burleigh, M. R., et al. 2011, MNRAS, 418, 1156
Merritt, D., Alexander, T., Mikkola, S., & Will, C. M. 2011, PhRvD, 84, 044024
Nelemans, G., Yungelson, L. R., Portegies Zwart, S. F., & Verbunt, F. 2001, A&A, 365, 491
Padmanabhan, T. 2001, Theoretical Astrophysics, Vol. 2, Stars and Stellar Systems (Cambridge: Cambridge Univ. Press), 594
Perets, H. B., Gualandris, A., Kupi, G., Merritt, D., & Alexander, T. 2009, ApJ, 702, 884
Peters, P. C. 1964, PhRv, 136, 1224
Press, W. H., & Teukolsky, S. A. 1977, ApJ, 213, 183
Prodan, S., & Murray, N. 2012, ApJ, 747, 4
Rauch, K. P., & Tremaine, S. 1996, NewA, 1, 149
Rees, M. J. 1988, Natur, 333, 523
Renzini, A., Greggio, L., di Serego Alighieri, S., et al. 1995, Natur, 378, 39
Sesana, A., Vecchio, A., Eracleous, M., & Sigurdsson, S. 2008, MNRAS, 391, 718
Shen, R.-F., & Matzner, C. D. 2014, ApJ, 784, 87
Stone, N., Sari, R., & Loeb, A. 2013, MNRAS, 435, 1809
Strubbe, L. E., & Quataert, E. 2009, MNRAS, 400, 2070
Strubbe, L. E., & Quataert, E. 2011, MNRAS, 415, 168
Ulmer, A. 1999, ApJ, 514, 180
van Velzen, S., Farrar, G. R., Gezari, S., et al. 2011, ApJ, 741, 73
Wang, J., & Merritt, D. 2004, ApJ, 600, 149
Wang, T.-G., Zhou, H.-Y., Komossa, S., et al. 2012, ApJ, 749, 115
Wang, T.-G., Zhou, H.-Y., Wang, L.-F., Lu, H.-L., & Xu, D. 2011, ApJ, 740, 85
Zalamea, I., Menou, K., & Beloborodov, A. M. 2010, MNRAS, 409, L25